PHYSICS AND CHEMISTRY OF SOLID STATE
V. 25, No. 1 (2024) pp. 51-56
Section: Technology

DOI: 10.15330/pcss.25.1.51-56

Vasyl StefanykPrecarpathian National University

ФІЗИКА І ХІМІЯ ТВЕРДОГО ТІЛА
Т. 25, № 1 (2024) С. 51-56
Технічні науки

PACS:61.43.Gt, 81.05.Rm ISSN 1729-4428

V.I. Mandzyuk[1], R.P. Lisovskiy[2], Yu.O. Kulyk[3], B.I. Rachiy[1], R.V. Solomovskyi[1]

The effect of thermal modification of turbostratic carbon on its fractal structure

[1]*Vasyl StefanykPrecarpathian National University, Ivano-Frankivsk, Ukraine, volodymyr.mandzyuk@pnu.edu.ua*
[2]*Ivano-Frankivsk National Medical University, Ivano-Frankivsk, Ukraine,*
[3]*Ivan Franko National University of Lviv, Lviv, Ukraine*

Fractal structure of porous carbon materials (PCMs) obtained by thermal modification under different regimes was investigated using the method of low-temperatureporometry. It was set that at modification temperatures of 300 and 600°C, materials with a developed microporous structure are formed, the surface fractal dimension of which is 2.64. When the modification temperatures are 400 and 500°C, the value of the fractal dimension of the surface decreases to a value of 2.22 with an increase in the duration of modification, which indicates the formation of an almost smooth surface as a result of the intensive removal of carbon atoms from the surface layers and a decrease in the number of micropores due to their transition into mesopores.

Keywords: porous carbon material, thermal modification, low-temperatureporometry, specific surface area, surface fractal dimension.

Received 04 October2023; Accepted 05February2024.

Introduction

The developed specific surface area of PCMs is one of the important parameters that makes their attractive for use in lithium power sources [1-3] and electrochemical capacitors [4-6] as an electrode material. During the carbonization of raw materials, it is quite difficult to obtain PCMs with a specific surface area more than 500 m^2/g and a total pore volume more than 0.2 cm^3/g. This determines the need for additional modification and treatment of such materials.

The main methods of PCMs modification and treatment include thermochemical methods [7-9], ultrasonic and laser treatment methods [10, 11], as well as the use of exo- and endotemplates [12-14]. When using the specified treatment methods, both the parameters of the porous structure of carbon materials (specific surface area, pore volume and their size distribution) change, and their fractal structure changes. Earlier, we have investigated the features of the fractal structure of PCMs obtained by hydrothermal carbonization of plant raw materials and determined how the value of the surface fractal dimension D_s changes as the carbonization temperature of the raw material increases [15]. The aim of this work is to study the effect of thermal modification regimes (temperature and time) of PCMs on their fractal structure using the method of low-temperature porometry.

I. Materials and methods

PCM obtained by hydrothermal carbonization of plant raw materials at a temperature of 750°C was the initial material for thermal modification [15]. To increase the specific surface due to the removal from the carbon matrix of the most reactive carbon atoms that interact with gasifying agents, PCM was placed in a chamber where it was kept for a given time in a gas flow (a mixture of hot air and argon). The main parameters of the process were the temperature t_{mod} and the modification time τ_{mod}. Thermal modification was carried out at temperatures of 300, 400, and 500°C for a duration of 0.5 ÷ 3 h and 600°C for a duration of 0.25 ÷ 1 h. In the latter case, shorter modification times of PCM are due to the fact that further heat treatment leads to complete burnout of the material at

a given temperature.

Quantachrome Autosorb (Nova 2200e) automatic sorbtometer was used to obtain sorption isotherms of PCMs at the boiling temperature of nitrogen (T = 77 K). Before measurements, the samples were degassed in a vacuum at 180°C for 20 hours. The Brunauer-Emmett-Teller (BET) method was used to determine the total specific surface area of pores S_{BET}, the specific surface area of micropores S_{micro} was determined by the t-method, the surface area of mesopores S_{meso} was calculated as the difference between the total surface area of pores and micropores [16].

The surface fractal dimension D_s of PCMs was determined by rearranging the nitrogen adsorption isotherm according to the equation [17]:

$$\ln\left(\frac{V}{V_{mono}}\right) = const + A\left[\ln\left(\ln\left(\frac{p_0}{p}\right)\right)\right], \qquad (1)$$

where V is the volume of adsorbed gas; V_{mono} is the volume of adsorbed gas that covers the surface of the sample with a monolayer; A is a degree indicator that depends on the surface fractal dimension D_s; p_0/p is the relative pressure. The volume of the monolayer coating V_{mono} was calculated according to the BET method [16]:

$$\frac{1}{W[(p_0/p)-1]} = \frac{1}{W_{mono}C} + \frac{C-1}{W_{mono}C}\cdot\frac{p}{p_0}, \qquad (2)$$

where W is the mass of gas adsorbed at the relative pressure p/p_0; W_{mono} is the mass of adsorbed matter which forms a monolayer that covers the entire surface; C is the BET-constant, which characterizes the adsorption energy in the first adsorption layer and is an indicator of the magnitude of the adsorbent/adsorbate interaction.

According to [18], van der Waals forces prevail at the interaction of PCMs and gas at the initial stage of nitrogen adsorption. Surface tension forces on the liquid-gas interface can be neglected. The relation between A and D_s parameters is given by the equality:

$$D_s = 3A + 3. \qquad (3)$$

During further adsorption, the forces of surface tension between gas and liquid begin to dominate. In this case, the ratio is fulfilled:

$$D_s = A + 3. \qquad (4)$$

It follows from equations (3) and (4) that the surface fractal dimension D_s of PCM can be determined based on the equation required for a specific case. The limit that determines the dominance of surface tension forces or van der Waals ones is given by the equation [18]:

$$\alpha = 3A + 1. \qquad (5)$$

Van der Waals forces prevail if $\alpha \geq 0$. When $\alpha < 0$, surface tension forces dominate.

II. Results and discussion

According to low-temperature porometry data (Fig. 1), the sorption isotherms for PCMs obtained by modification at 300°C at all modification times are the same in shape and belong to the I type of isotherms, which is typical for microporous materials (Fig. 1, curve 2). There is a low-pressure hysteresis on these isotherms, which is less expressed compared to the initial material. The most probably reason for this behavior may be a decrease in the irreversible retention of nitrogen molecules in pores, the size of which is proportional to the size of nitrogen molecules, due to the appearance of oxygen-containing functional groups on the surface of carbon particles. For these materials, the amount of adsorbed gas is somewhat greater than for the initial sample.

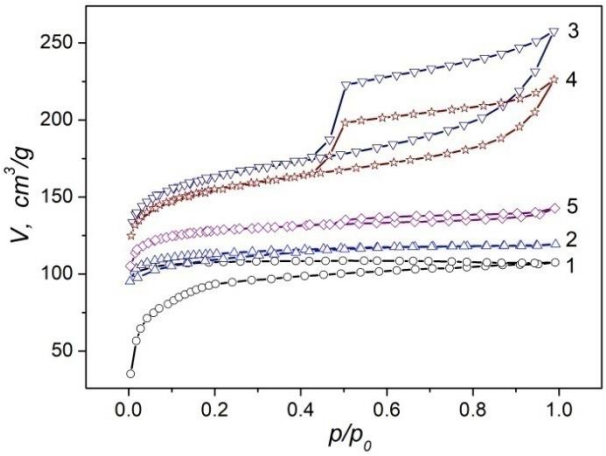

Fig. 1. Nitrogen sorption isotherms for initial (1) and modified at temperatures of 300°C (2), 400°C (3), 500°C (4), and 600°C (5) PCMs.

For PCM modified at 400°C for 0.5 h the isotherm is a similar kind. However, at τ_{mod} = 1 ÷3 h and t_{mod} = 500°C for all modification times, the form of the isotherms changes sharply. In the range of relative pressures p/p_0 = 0.42 ÷ 1, high pressure hysteresis is present on the isotherms. According to the IUPAC classification, this hysteresis belongs to the H4 type [16] and is associated with capillary condensation in mesopores (Fig 1, curves 3 and 4). When the duration of modification increases, the value of hysteresis increases and is ΔV = 3÷43 cm^3/g for t_{mod} = 400°C and ΔV = 8 ÷ 31 cm^3/g for t_{mod} = 500°C. There is no low-pressure hysteresis in these samples.

For PCMs obtained at a modification temperature of 600°C, the sorption isotherm (Fig. 1, curve 5) is similar to curves 3 and 4. However, due to shorter modification times, the high-pressure hysteresis is less expressed and is ΔV = 3 cm^3/g at p/p_0 = 0.7. There is no hysteresis at τ_{mod} = 1 h, which indicates the formation of a microporous material.

Presenting the adsorption isotherms in the coordinates $\ln(V/V_{mono}) = f\{\ln[\ln(p_0/p)$ (Fig. 2) and using formulas (3)-(5) to calculate the surface fractal dimension D_s, it is possible to set how the value D_s changes during thermal modification of PCMs.

As can be seen from Fig. 2, linear regions with different inclination angles are observed on the obtained dependences, which indicate the large-scale properties of

the surface of the materials. When the relative pressure increases, the number of nitrogen molecules adsorbed in the pores increases. As a result, the interface between the adsorbent and the adsorbate becomes smoother. In this case, the D_s parameter no longer describes the solid-gas interface, but characterizes the interaction of the material surface with polyatomic layers of adsorbed nitrogen molecules. Therefore, the first linear region was chosen to correctly determine the surface fractal dimension of the PCMs.

According to the calculations (Table 1), the parameter α has a positive value for all PCMs, which indicates the dominance of van der Waals forces in the adsorbent-adsorbate system and the need to use equality (3) to find the fractal dimension of the surface D_s.

As follows from the Table 1, the fractal dimension of the surface increases at a modification temperature of 300°C. The main reason for this growth is an increase in the portion of micropores in relation to the initial material (according to Table 2, the portion of the micropore surface increases to 95%). However, this temperature is insufficient for the formation of a developed mesoporous structure, for which the value of the surface fractal dimension is smaller. Similarly, shorter modification times of the initial material at 600°C almost do not change the dimension of the surface, although the number of micropores, as in the previous case, increases to 96 % (Table 2). This is due to the compaction of the structure of carbon particles due to the compaction of microregions formed by graphene layers.

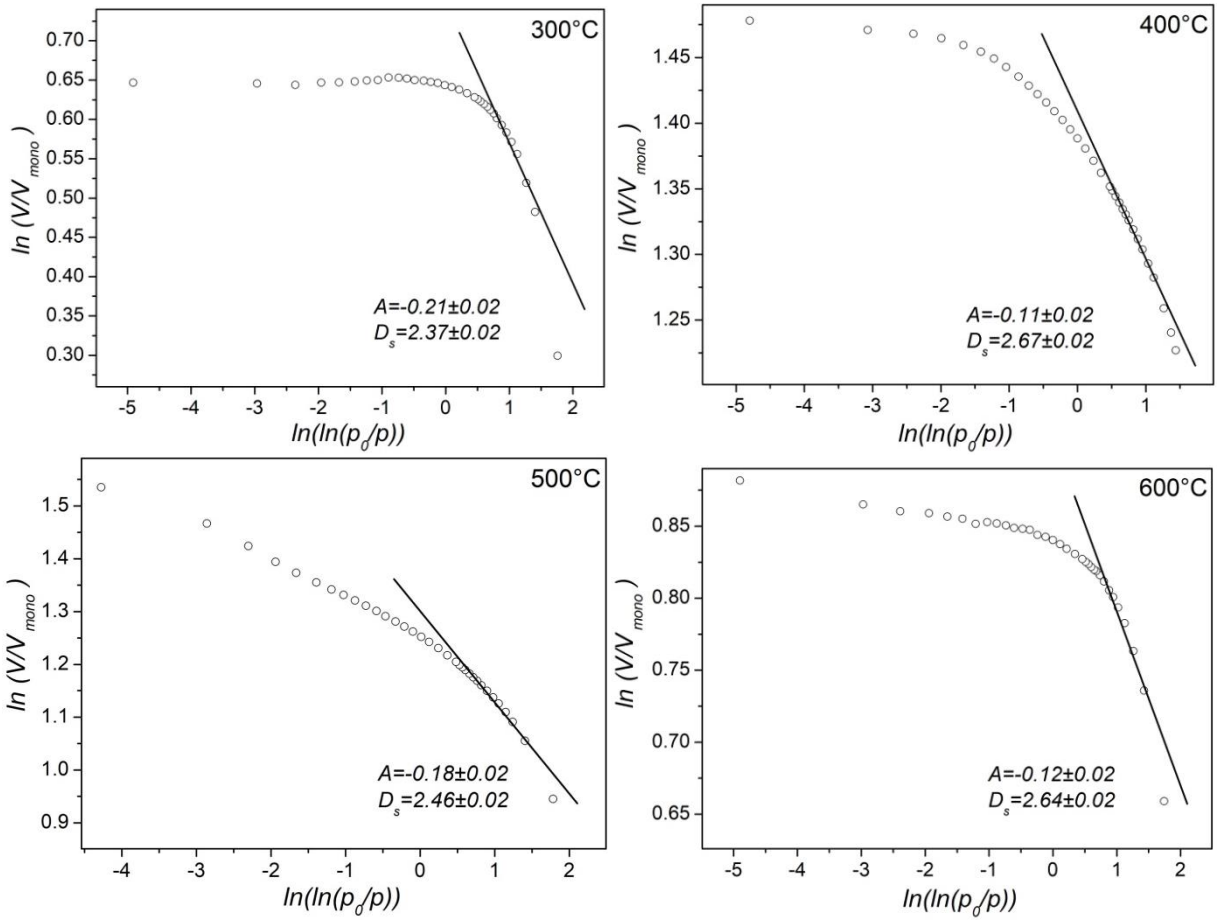

Fig. 2. Dependences $\ln(V/V_{mono}) = f\{\ln[\ln(p_0/p)]\}$ for PCMs obtained at different modification temperatures at τ_{mod} = 1 h.

Table 1.

Parameters of the fractal structure of thermally modified PCMs

τ_{mod}, h	t_{mod} = 300°C			t_{mod} = 400°C			t_{mod} = 500°C			t_{mod} = 600°C		
	A	*α*	D_s	*A*	*α*	D_s	*A*	*α*	D_s	*A*	*α*	D_s
0.25										-0.14	0.58	2.58
0.5	-0.26	0.22	2.22	-0.09	0.73	2.73	-0.16	0.52	2.52	-0.13	0.61	2.61
0.75										-0.13	0.61	2.61
1	-0.21	0.37	2.37	-0.11	0.67	2.67	-0.18	0.46	2.46	-0.12	0.64	2.64
1.5	-0.13	0.61	2.61	-0.18	0.46	2.46	-0.20	0.40	2.40			
2	-0.12	0.64	2.64	-0.19	0.43	2.43	-0.22	0.34	2.34			
2.5	-0.12	0.64	2.64	-0.22	0.34	2.34	-0.24	0.28	2.28			
3	-0.11	0.67	2.67	-0.26	0.22	2.22	-0.26	0.22	2.22			

for the initial material$A$ = –0.45; α = –0.35; D_s = 2.55.
the absolute error in determining the parameters is ± 0.02.

Table 2.

Parameters of the porous structure of thermally modified PCMs

t_{mod}, °C	τ_{mod}, h	S_{BET}, m^2/g	S_{micro}, m^2/g	S_{meso}, m^2/g	S_{micro}/S_{BET}, %
initial	–	343	292	51	86
300	0.5	361	339	51	94
	1	443	425	18	96
	1.5	434	410	24	95
	2	439	418	21	95
	2.5	451	424	27	94
	3	450	423	27	94
400	0.5	433	380	53	88
	1	513	453	60	88
	1.5	542	478	74	88
	2	573	500	73	87
	2.5	614	504	110	82
	3	652	535	117	82
500	0.5	526	463	63	88
	1	623	522	101	84
	1.5	616	519	97	84
	2	653	550	103	84
	2.5	586	492	94	84
	3	479	404	75	84
600	0.25	465	411	54	88
	0.5	497	464	33	93
	0.75	464	441	23	95
	1	457	439	18	96

For modification temperatures of 400 and 500°C, there is a tendency for the D_s parameter to decrease with increasing duration of modification, which indicates the formation of an almost smooth surface. A similar situation for the given temperatures was observed when studying these materials by the method of small-angle X-ray scattering (SAXS) (Table 3), the use of which made it possible to determine the value of the surface fractal dimension of both open and closed pores [19].

Comparing the data of SAXS and low-temperature porometry (Table 4), it is also possible to estimate the portion of the specific surface of open pores k in PCM relative to the entire surface of the material. In this case, open pores include pores on the surface of which nitrogen molecules are adsorbed.

As follows from the data in the Table 4, the most significant development of the open porous structure is observed as a result of thermal modification at temperatures of 400 and 500°C. Thermal modification at 300°C is insufficiently effective for the formation of a mesoporous structure. It is possible that the micropores are closed by reaction products at this temperature, which also limits the access of nitrogen molecules to this part of the PCM. For the samples modified at 600°C, the main reason for the decrease in the parameter k is probably the compaction of the PCM structure. This, in turn, leads not only to an increase in microporosity, but also to the formation of ultra-micropores and the closing of some open pores.

Thus, adjusting the temperature and time of modification of the initial material, it is possible to obtain PCMs with a controlled porous structure and fractal dimension, which is an effective tool in the synthesis of materials with predetermined properties.

Table 3.

D_s value according to SAXS and low-temperature porometry

τ_{mod}, h	t_{mod} = 300°C		t_{mod} = 400°C		t_{mod} = 500°C		t_{mod} = 600°C	
	D_s^*	D_s^{**}	D_s^*	D_s^{**}	D_s^*	D_s^{**}	D_s^*	D_s^{**}
0.25							2.6	2.58
0.5	2.2	2.22	2.8	2.73	2.5	2.52	2.55	2.61
0.75							2.6	2.61
1	–	2.37	2.7	2.67	2.4	2.46	2.6	2.64
1.5	2.3	2.61	2.4	2.46	2.2	2.40		
2	2.3	2.64	2.2	2.43	2.0	2.34		
2.5	2.7	2.64	2.1	2.34	2.0	2.28		
3	2.7	2.67	2.0	2.22	2.0	2.22		

* SAXS data [19]; **low-temperature porometry data.
for the initial material $D_s^* = 2.6$; $D_s^{**} = 2.55$.

Table 4.

Specific surface area of PCMs according to SAXS [19] and BET-method

τ_{mod}, h	t_{mod} = 300°C			t_{mod} = 400°C			t_{mod} = 500°C			t_{mod} = 600°C		
	S_{SAXS}	S_{BET}	k	S_{SAXS}	S_{BET}	k	S_{SAXS}	S_{BET}	k	S_{SAXS}	S_{BET}	k
0.25										777	465	60
0.5	785	361	46	634	433	68	665	526	79	788	497	63
0.75										853	464	54
1	729	443	61	657	513	78	774	623	80	847	457	54
1.5	805	434	54	694	542	78	767	616	80			
2	773	439	57	734	573	78	806	653	81			
2.5	755	451	60	832	614	79	915	586	64			
3	768	450	59	795	652	82	912	479	53			

specific surface area in m^2/g;
k in % (for the initial material k = 73 %).

Conclusions

The possibility of using the low-temperature porometry method for studying the fractal structure of PCMs obtained under different conditions of thermal modification is shown. The surface fractal dimension of PCMs is greater than that of the initial material at modification temperatures of 300 and 600°C due to an increase in the proportion of the specific surface area of micropores relative to the total specific surface area of pores. When modification temperarure are 400 and 500°C and the duration of modification increases, there is the redistribution between micro- and mesopores in the direction of an increase in the number of mesopores, which leads to the formation of an almost smooth surface of materials with a surface fractal dimension close to 2. A comparative analysis was carried out between the data of low-temperature porometry and small-angle X-ray scattering, which indicates a correlation in the change in the value D_s.

Mandzyuk V.I. – Doctor in Physics and Mathematics, Professor of Department of Computer Engineering and Electronics;
Lisovskiy R.P. – Doctor in Physics and Mathematics, Professor of Department of Medical Informatics, Medical and Biological Physics;
Kulyk Yu.O. – PhD in Physics and Mathematics, Leading Engineer of Department of Metal Physics;
Rachiy B.I. – Doctor in Physics and Mathematics, Professor of Department of Materials Science and Advanced Technologies;
Solomovskyi R.V. – PhD Student, Department of Computer Engineering and Electronics.

[1] Z. Guan, Z. Guan, Z. Li, J. Liu, K. Yu, *Characterization and preparation of nanoporous carbon derived from hemp stems as anode for lithium-ion batteries*, Nanoscale Research Letters, 14, 338 (2019); https://doi.org/10.1186/s11671-019-3161-1.
[2] Y. Dou, X. Liu, K. Yu, X. Wang, W. Liu, J. Liang, C. Liang, *Biomass porous carbon derived from jute fiber as anode materials for lithium-ion batteries*, Diamond and Related Materials, 98. 107514 (2019); https://doi.org/10.1016/j.diamond.2019.107514.
[3] V.I. Mandzyuk, V.A. Povazhnyi, B.I. Rachiy, *Anthracite-derived porous carbon as electrode material of lithium power sources*, Journal of Nano- and Electronic Physics, 10(4), 04033 (2018); https://doi.org/10.21272/jnep.10(4).04033.
[4] D.S. Priya, L.J. Kennedy, G.T. Anand, *Emerging trends in biomass-derived porous carbon materials for energy storage application: A critical review*, Materials Today Sustainability, 21, 100320 (2023); https://doi.org/10.1016/j.mtsust.2023.100320.
[5] Z. Pan, S. Yu, L. Wang, C. Li, F. Meng, N. Wang, S. Zhou, Y. X, Z. Wang, Y. Wu, X. Liu, B. Fang, Y. Zhang, *Recent advances in porous carbon materials as electrodes for supercapacitors*, Nanomaterials, 13(11), 1744 (2023); https://doi.org/10.3390/nano13111744.
[6] A.I. Kachmar, V.M. Boichuk, I.M. Budzulyak, V.O. Kotsyubynsky, B.I. Rachiy, R.P. Lisovskiy, *Effect of synthesis conditions on the morphological and electrochemical properties of nitrogen-doped porous carbon materials*, Fullerenes Nanotubes and Carbon Nanostructures, 27(9), 669 (2019); https://doi.org/10.1080/1536383X.2019.1618840.
[7] J. Zhou, A. Luo, Y. Zhao, *Preparation and characterisation of activated carbon from waste tea by physical activation using steam*, Journal of the Air & Waste Management Association, 68(12), 1269 (2018); https://doi.org/10.1080/10962247.2018.1460282.
[8] M. Härmas, T. Thomberg, H. Kurig, T. Romann, A. Jänes, E. Lust, *Microporouse mesoporous carbons for energy storage synthesized by activation of carbonaceous material by zinc chloride, potassium hydroxide or mixture of them*, Journal of Power Sources, 326, 624 (2016);https://doi.org/10.1016/j.jpowsour.2016.04.038.
[9] Yu. Starchuk, N. Ivanichok, I. Budzulyak, S.-V. Sklepova, O. Popovych, P. Kolkovskyi, B. Rachiy, *Electrochemical properties of nanoporous carbon material subjected to multiple chemical activation*, Fullerenes Nanotubes and Carbon Nanostructures, 30(9), 936 (2022); https://doi.org/10.1080/1536383X.2022.2043285.
[10] G. Zhou, J. Yin, Z. Sun, X. Gao, F. Zhu, P. Zhao, R. Lia, J. Xu, *An ultrasonic-assisted synthesis of rice-straw-based porous carbon with high performance symmetric supercapacitors*, RSC Advances, 10(6), 3246 (2020); https://doi.org/10.1039/c9ra08537h.
[11] H. Hu, Q. Li, L. Li, X. Teng, Z. Feng, Y. Zhang, M. Wu, J. Qiu,*Laser Irradiation of Electrode Materials for Energy Storage and Conversion*, Matter, 3(1), 95 (2020); https://doi.org/10.1016/j.matt.2020.05.001.
[12] W. Cha, S. Kim, P. Selvarajan, J.M. Lee, J.M. Davidraj, S. Joseph, K. Ramadass, I.Y. Kim, A. Vinu, *Nanoporous carbon oxynitride and its enhanced lithium-ion storage performance*, Nano Energy, 82, 105733 (2021); https://doi.org/10.1016/j.nanoen.2020.105733.
[13] V.I. Mandzyuk, I.F. Myronyuk, V.M. Sachko, I.M. Mykytyn, *Template synthesis of mesoporous carbon materials for electrochemical capacitors*, Surface Engineering and Applied Electrochemistry, 56(1), 93 (2020); https://doi.org/10.3103/S1068375520010123.
[14] L. Xie, Z. Jin, Z. Dai, Y. Chang, X. Jiang, H. Wang. *Porous carbons synthesized by templating approach from fluid precursors and their applications in environment and energy storage: A review*, Carbon, 170, 100 (2020); https://doi.org/10.1016/j.carbon.2020.07.034.

[15] V.I. Mandzyuk, R.P. Lisovskiy, *Fractal structure of nanoporous carbon obtained by hydrothermal carbonization of plant raw materials*, Journal of Nano- and Electronic Physics, 14(5), 05027 (2022); https://doi.org/10.21272/jnep.14(5).05027.
[16] S.J. Gregg, K.S.W. Sing, Adsorption, surface area and porosity (Academic, London,1982).
[17] P. Pfeifer, K.-Y. Liu, *Multilayer adsorption as a tool to investigate the fractal nature of porous adsorbents*, Studies in Surface Science and Catalysis, 104, 625 (1997); https://doi.org/10.1016/S0167-2991(97)80075-4.
[18] I.M.K. Ismail, P. Pfeifer, *Fractal analysis and surface roughness of nonporous carbon fibers and carbon black*, Langmuir, 10(5), 1532 (1994); https://doi.org/10.1021/la00017a035.
[19] B.K. Ostafiychuk, V.I. Mandzyuk, Yu.O. Kulyk, N.I. Nagirna, *SAXS investigation of nanoporous structure of thermal-modified carbon material*, Nanoscale Research Letters, 9(1), 160 (2014); https://doi.org/10.1186/1556-276X-9-160.

В.І. Мандзюк[1], Р.П. Лісовський[2], Ю.О. Кулик[3], Б.І. Рачій[1], Р.В. Соломовський[1]

Вплив термічної модифікації турбостратного вуглецю на його фрактальну структуру

[1]Прикарпатський національний університет імені Василя Стефаника, Івано-Франківськ, Україна, volodymyr.mandzyuk@pnu.edu.ua
[2]Івано-Франківський національний медичний університет, Івано-Франківськ, Україна
[3]Львівський національний університет імені Івана Франка, Львів, Україна

Методом низькотемпературної порометрії досліджено фрактальну структуру пористих вуглецевих матеріалів (ПВМ), отриманих термічною модифікацією при різних режимах. Встановлено, що за температур модифікації 300 і 600°C формуються матеріали з розвиненою мікропористою структурою, поверхнева фрактальна розмірність яких становить 2,64. За температур модифікації 400 і 500°C значення фрактальної розмірності поверхні зменшується до значення 2,22 при збільшенні тривалості модифікації, що свідчить про формування майже гладкої поверхні, що зумовлено інтенсивним видаленням атомів карбону з приповерхневих шарів та зменшенням кількості мікропор за рахунок їх переходу в мезопори.

Ключові слова: пористий вуглецевий матеріал, термічна модифікація, низькотемпературна порометрія, питома поверхня, поверхнева фрактальна розмірність.